Growth and morphology of partial and multilayer Fe thin films on Cu(100) and the effect of adsorbed gases studied by scanning tunneling microscopy

K. E. Johnson, D. D. Chambliss, R. J. Wilson, and S. Chiang
IBM Research Division, Almaden Research Center, San Jose, California 95120-6099

(Received 9 November 1992; accepted 25 January 1993)

Fe epitaxy on Cu(100) is investigated for Fe coverages $\theta \leqslant 3.0$ ML. The layer filling statistics are quantitatively related to an evolving growth process, which includes intermixing at the substrate overlayer interface. The resulting inhomogeneous substrate surface and first layer affect the processes by which arriving Fe atoms add to the growth front. Our results explain the previously reported covering of initial Fe not as bilayer growth, but instead as the result of island growth on top of Fe incorporated in the top substrate layer. First layer composition and structure influence the nucleation and growth of the second layer. Island coalescence and formation of a first layer percolation network change the connected first layer area thereby changing the nucleation and growth behavior of the second layer. After both first and second layer growth are completed, images show additional growth is much more layer-by-layer in nature. Oxygen exposure after Fe deposition changes the layer filling by both promotion of step crossing and expansion of partially filled Fe layers.

I. INTRODUCTION

Nonequilibrium metal on metal epitaxial growth and the resulting structures are not readily probed with single techniques. Periodic structure revealed by diffraction, and composition from spectroscopy, are well complemented by real space imaging using scanning tunneling microscopy (STM). The structure of the initial deposition of Fe on Cu(100) is of particular interest for deposition below $\theta \approx 10$ monolayers (ML) because of the stabilization of fcc iron and the resultant magnetic properties.[1] The quality of the interface between the Cu substrate and Fe overlayer affects the magnetic properties of very thin layers and sandwich structures, but studies to date do not provide a complete or accurate picture of the microscopic growth structures and mechanism in this very low coverage regime.

As our measurements were made for room-temperature (RT) deposition, previous results for the Fe on Cu(100) system made under comparable conditions will be discussed here. Results from Auger electron diffraction (AED)[2] and x-ray photoelectron diffraction (XPD)[3] show forward scattering anisotropies after submonolayer Fe deposition. This implies that Fe atoms are already covered by either Fe or Cu at this stage of deposition. Another study correlated Fe/Cu intensity ratios in Auger electron spectroscopy (AES) with Fe coverage calibrated using Rutherford backscattering, and assigned breakpoints to the completion of 2 and 4 ML.[4] Both of these results have been interpreted as evidence for sequential growth of bilayers for deposition of $\theta \leqslant 4$ ML. Contradicting this model are results using CO adsorption to titrate the surface composition.[3] Even after $\theta > 2$ ML Fe deposition, Cu atoms remain exposed. Diffraction intensity measurements during initial epitaxial growth using reflection high-energy electron diffraction (RHEED),[5] medium-energy electron diffraction (MEED),[6] and helium atom scattering (HAS)[7] also contradict a simple ordered growth mechanism. Deposition of the initial 1 ML of Fe reduces the specular diffraction intensity, which only partially recovers by $\theta \cong 4$ ML when simple 1 ML period oscillations begin. Again these results are interpreted as evidence for multilayer agglomeration but not necessarily formation of bilayers. Layer-by-layer growth is ultimately achieved, but only after completion of an initial deposited layer, the structure of which is not adequately explained by any of the previously mentioned studies. At higher coverages, the oscillations damp out as added material reverts to the bulk bcc Fe structure, and low-energy electron diffraction (LEED) indicates a change in the ordering of the overlayer.

The atomic structures that result from epitaxy are controlled by both the thermodynamics of the substrate and deposited material, and by the kinetics of atomic motion and addition at the surface. The resulting growth structures in turn influence the kinetics of further deposition. Figure 1 suggests some of the possible atomic motions during deposition. The thermodynamic limits for initial growth are either wetting of the surface by arriving atoms, or agglomeration into multilayer structures. Kinetic limitations involving atom mobility, island nucleation, and step crossing determine the actual result for the nonequilibrium conditions of deposition. Figure 1(a) illustrates the case for layer-by-layer growth where step crossing allows for atoms arriving on top of first layer growth to step down and add at edges of existing growth. The competition between nucleation and diffusion determines whether this type of epitaxy is by step flow or island nucleation and aggregation. Figure 1(b) illustrates thermodynamically preferred bilayer growth, as proposed for Fe epitaxy on Cu(100).[4] If agglomeration is to occur, some arriving atoms must step up at edges of existing growth. When step crossing is kinetically unfavorable, arriving atoms are trapped on the layer where they arrive, as depicted in Fig.

 0734-2101/93/11(4)/1654/7/$1.00

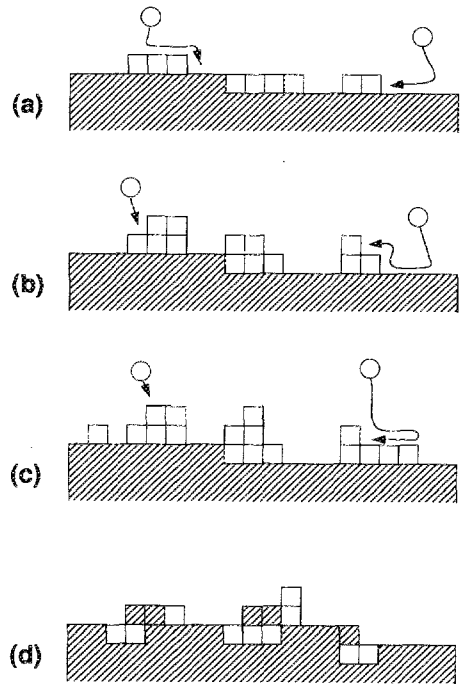

FIG. 1. Schematic representation of possible growth modes. (a) Layer-by-layer growth. Arriving atoms step down off existing first layer growth. First layer growth can occur either via step-flow or island nucleation. (b) Bilayer agglomeration. Arriving atoms tend to grow with thermodynamic driving force into double height layer. (c) Multilayer growth promoted by kinetically inhibited step crossing. (d) Possible growth structure resulting from intermixing of arriving atoms with the top layer of the substrate.

1(c). In the extreme, this leads to a Poisson distribution of exposed layers. The final illustration, Fig. 1(d), suggests that epitaxy that includes thermodynamically driven intermixing at the initial growth interface can have profound consequences in the initial stages of growth.

In spite of the considerable experimental evidence available for the Fe/Cu(100) epitaxial system, an understanding of the atomic mechanisms and resulting structures for the initial growth is lacking. STM provides the means to measure the details of structure unambiguously, and in some cases with important compositional information. Specifically, bilayer growth mechanisms can be immediately and unambiguously observed if actually present. For example, STM measurements of Au on Ag(110) epitaxy have recently shown that the growth mode is not bilayer formation, but rather is one in which the first ML of Au resides in the substrate under the top layer of Ag atoms.[8] In the case of Fe epitaxy on Cu(100), STM can measure both the microscopic composition and the mesoscopic structure of the exposed surface as it changes with increasing growth. From this we can infer the changes in the mode by which arriving Fe atoms are incorporated.

We will address the atomic behavior of Fe deposition for $\theta \leqslant 3.0$ ML, specifically relating layer filling and composition to the measured structure. Following is a discussion of how oxygen exposure after deposition changes the surface structure, and selectively decorates iron.

II. EXPERIMENTAL

The experiment was performed using a STM incorporated in a multichamber ultrahigh vacuum system.[9] The Cu(100) single crystal was prepared by standard Ar ion sputtering and annealing to ≈ 600 °C. All depositions reported herein, with a single noted exception, were performed after the sample was allowed to cool at least 1 h; we estimate that the sample had cooled by radiation and conduction to within 20° of RT. The deposition source consisted of a 99.998% pure Fe wire heated by electron bombardment. Deposition rates used were 0.2–1.0 ML/min. A single deposition was performed at 0.03 ML/min as a check for background contamination. Insignificant carbon contamination frequently accompanied Fe deposition, as detected by AES at $<0.2\%$. Absolute coverage of deposited Fe was determined from the STM images. For thicker layers, the inherent uncertainty from defining the absolute layer height in an image was overcome using Fe/Cu AES ratios. To monitor the Fe flux to the sample during deposition, an ion gauge was placed in line with the Fe source but not shadowing the sample. The integrated increase in the pressure reading during deposition provided an accurate ($\pm 2\%$) means to control coverage.

Imaging was in the constant current mode, with currents of 1.0–2.0 nA. Sample bias only affected topography for images taken at coverages $\theta < 0.4$ ML. Images are shown in height keyed gray scale with a quadratic background subtracted and linear skew to correct drift during scanning. Quantitative analysis of layer occupation was performed on selected regions of images, specifically avoiding terrace edges where original edge boundaries are ambiguous. Intensity thresholds for each layer were assigned and the fractional areas at each level calculated. Every effort was made to minimize the effect of tip shape in this image analysis.

III. Fe on Cu(100)

A. Results

Some immediate qualitative conclusions can be reached after examining the mesoscopic structure of layer growth shown at the three coverages in Fig. 2. At Fe coverage $\theta = 0.23$ ML, Fig. 2(a) shows the surface morphology consists principally of first layer islands with a broad distribution of sizes. Some small islands of second layer growth have begun to nucleate on top of these first layer islands, but at less than 3% of the first layer coverage. This immediately contradicts a bilayer growth mechanism. Figure 2(b) shows the surface after deposition of $\theta = 1.3$ ML of Fe. At this coverage a substantial fraction, $\approx 15\%$, of the substrate is still exposed. The total growth is distributed 63% in the first layer and 37% in the second layer; less than 1% growth is observed for third layer islands. This distribution is far from ideal layer-by-layer growth, nor is it a Poisson distribution. At higher coverage, $\theta = 2.8$ ML in Fig. 2(c), the layer filling is closer to ideal. At this coverage $\approx 96\%$ of the growth front is in the third layer, that which is being completed at this stage. Coverage in the fourth layer is $<4\%$ that of the third. The image also

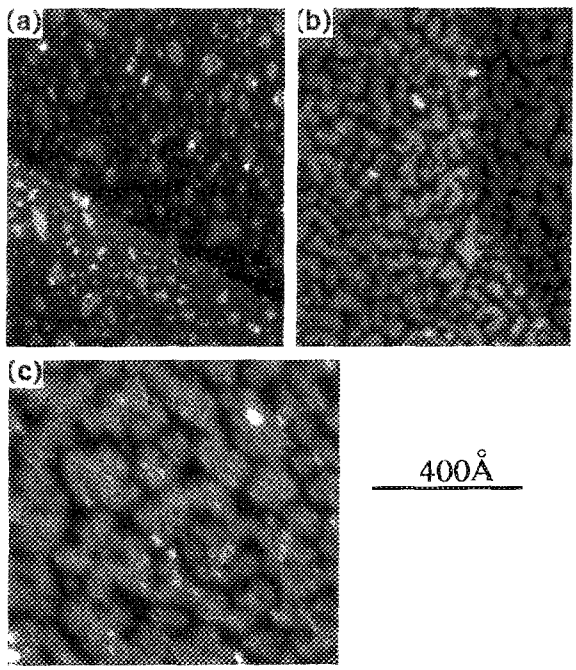

FIG. 2. STM images of mesoscopic surface structure after deposition of Fe on Cu(100). (a) Initial growth at $\theta = 0.23$ ML. Majority of growth is first layer single atomic height islands with $<3\%$ second layer growth nucleated. $i_{\text{tunnel}} = 0.8$ nA, $V_{\text{sample}} = -1.0$ V. (b) Structure after more than 1 ML deposition, $\theta = 1.3$ ML. Growth is distributed between first and second layers with only a few small third layer islands. $i_{\text{tunnel}} = 2.0$ nA, $V_{\text{sample}} = +0.2$ V. (c) Growth imaged after completion of first 2 ML, $\theta = 2.8$ ML. Here growth is primarily in the nearly complete third layer with concurrent change in characteristic size. $i_{\text{tunnel}} = 1.0$ nA, $V_{\text{sample}} = +1.0$ V.

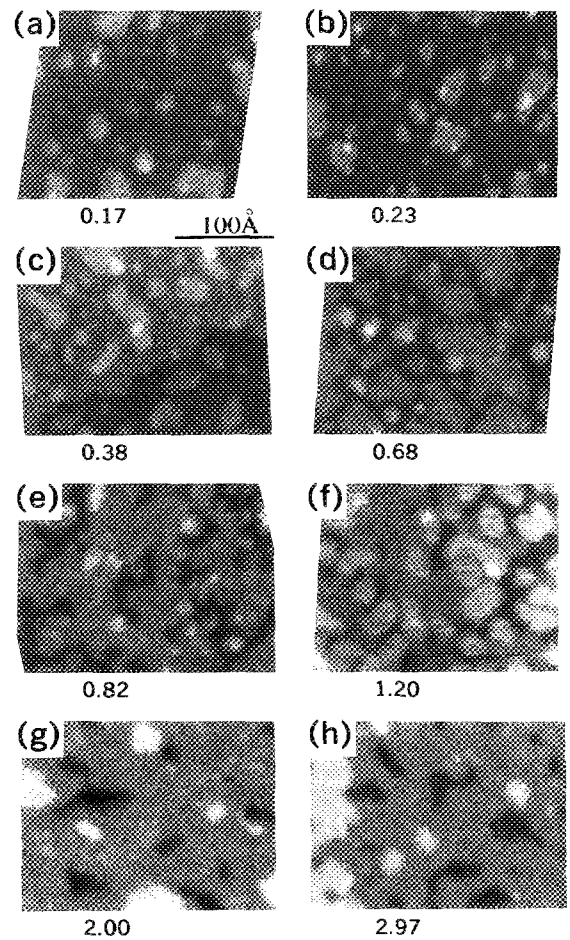

FIG. 3. Island nucleation and growth as imaged at different stages of Fe deposition. Coverage is noted in the figure. Most islands are monolayer high. Note the changing island shapes in (a) through (d). Island density continues to increase until coalescence becomes significant at coverages imaged in (c). A first layer percolation network is imaged at the coverage shown in (e). (f) shows presence of incomplete first and second layer growth. (g) and (h) exhibit a more layer-by-layer appearance.

shows a clear increase in the characteristic length scale of surface features by approximately a factor of 2.

In order to quantify the layer growth behavior of Fe on Cu(100), we have imaged the resulting growth front after deposition of Fe coverages from $\theta = 0.11$ ML to $\theta = 2.97$ ML. Figure 3 is a selection of images from this series. Using images such as these we can measure fractional area exposed for each layer, and calculate the fractional completion of each layer. These are the data plotted in Fig. 4(a), with dashed lines suggesting the changing trends in the growth behavior. A statistical measure of islands is also possible. In Fig. 4(c), the density of first layer islands is plotted. The maximum in density indicates island nucleation continues and the number of islands increases until the coverage becomes sufficiently high that the rate at which islands coalesce exceeds that for the nucleation of new islands. Where the density plot stops, coalescence has created a completely interconnected first layer. The filling of subsequent layers depends on the nature of layers already present on the surface growth front.

The broad distribution of first layer island size seen in Fig. 2(a) and the continued nucleation of first layer islands indicated by measured island density in Fig. 4(c) suggests the interaction between first layer growth and the substrate is spatially inhomogeneous. The nature of this inhomogeneity becomes clear in Fig. 5. At Fe coverages $\theta \lesssim 0.3$ ML, STM images frequently show on the Cu substrate small patches which appear as holes, or less frequently as bumps.[10] Figure 5(a) is an image taken after $\theta = 0.19$ ML Fe deposition at RT. The patches have typical sizes 5–10 Å. The apparent depth, or height, is variable, depending on the tunneling bias and polarity, and on the nature of the probe tip. We interpret this heterogeneity of the substrate surface to be the result of Fe exchange with surface Cu atoms producing Fe inclusions in the top surface layer. The measured total area of these patches agrees with that measured for first layer island growth to within the errors inherent in the imaging method and interpretation. The origin of the sensitivity of the tunneling junction to the surface composition is unknown. The variable nature of this imaging mechanism suggests that electronic properties of the clean metal surface, tunneling barrier and density of states, are not responsible. More probable is the possibility that adsorbed gases on either the tip or surface change the local electronic structure at the substrate patches. Our results, however, provide no conclusive evidence for this conjecture.

We have performed two tests to check the consistency

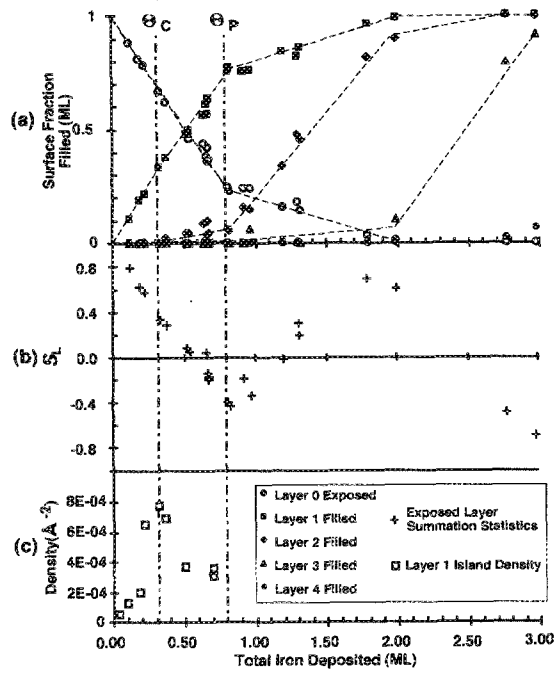

FIG. 4. Statistical data derived from images taken after varying amounts of Fe deposition. Coverages where first layer structure changes are indicated by vertical dashed lines. θ_C indicates where island coalescence predominates over nucleation, and θ_P formation of first layer percolation network. (a) Layer filling. The fraction of each atomic layer filled is plotted as a function of total Fe deposited. See legend for key to symbols for each layer. Dashed lines follow decrease in exposed substrate, and increases in layers 1–3. (b) Layer structure factor derived from exposed area at each level. This simulates antiphase diffraction intensity from layer occupation (see text). (c) First layer island density. At percolation threshold first layer growth becomes completely interconnected.

of our assumption that the patches are indeed Fe inclusions. First, Fe deposition onto a substrate heated at 80 ±15 °C yields results very similar to RT deposition, but with a number density of Fe patches that is 30% lower (Fig. 5). The mean area of patches is larger by the same factor. This is consistent with nucleation and growth of Fe inclusions and thermal activation of diffusion for arriving Fe atoms. In a separate experiment to check the possibility that gas contaminants during deposition are the source of the imaged patches, we deposited $\theta = 0.04$ ML at a rate of 0.03 ML /min. Thus, the sample was exposed to any contaminants emanating from the Fe source for 10× longer than at our usual deposition rates. Images taken after this deposition show no evidence of increased area or changed appearance in the patches. Considering these results, and that patches are only observed after Fe deposition, we must conclude that we are imaging the heterogeneous substrate top layer.

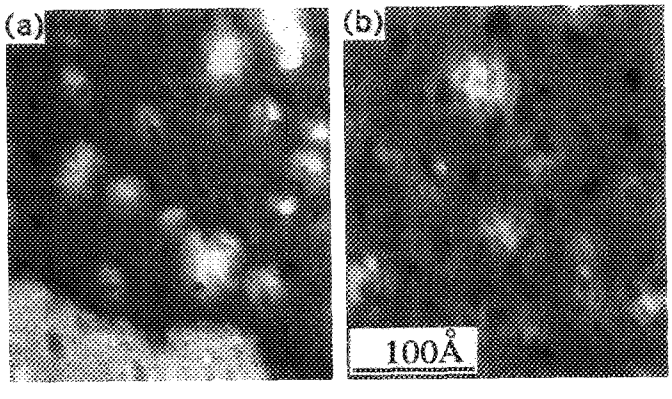

FIG. 5. Fe substrate inclusions. Small patches of Fe in substrate top atomic layer are reproducibly imaged, usually as depressions. (a) RT deposition of $\theta = 0.19$ ML Fe. Patch density is measured at 1.3×10^{-3} Å^{-2}. The total patch area is roughly equivalent to the measured first layer filling. $i_{\text{tunnel}} = 1.0$ nA, $V_{\text{sample}} = +0.5$ V. (b) Patches imaged after deposition of $\theta = 0.15$ ML Fe with substrate at elevated temperature, $T = 80 \pm 15$ °C. Patch density is lower at 7.7×10^{-4} Å^{-2}. $i_{\text{tunnel}} = 1.0$ nA, $V_{\text{sample}} = +1.0$ V.

If Fe inclusions form in the substrate top layer then first layer growth must be at least partially from the ejected Cu atoms. The heterogeneity of the first layer is apparent from the patches imaged on islands in Figs. 5(a) and 5(b). Additional evidence of inhomogeneity in the initial deposition is observed on exposed growth surfaces after deposition of up to 3 ML Fe. Mottling with height variations ~0.2 Å and typical length scale 6–10 Å is explained by Fe deposition on underlying layers with nonuniform composition.[10]

B. Discussion

The layer filling behavior combined with the observed inhomogeneity of submonolayer deposition provides the clues to understanding the atomic motions which generate the first layers of Fe epitaxy on Cu(100). The presence of distinct regions on the substrate, and the nonalloying behavior of bulk Fe–Cu systems, lead us to conclude that the patches observed in Fig. 5 are surface layer inclusions of essentially pure iron within the top atomic layer of the substrate. In this case, the behavior is distinct from that observed for Au on Cu(100) where a surface alloy is formed.[11] This implies that the initial process of RT Fe epitaxy on Cu(100) is an exchange of incoming Fe atoms with surface Cu atoms. The formation of distinct patches indicates that newly arrived Fe atoms must diffuse either on the surface or within the top substrate layer until a new inclusion is nucleated or the atom incorporates in a preexisting inclusion. Images from the deposition at elevated temperature, Fig. 5(b), show that nucleation and growth of the inclusions is influenced by thermally activated diffusion.

The material that first forms as first-layer growth consists of the Cu atoms ejected by the Fe–Cu exchange. These atoms form islands, except near steps where incorporation into the step above or below is more likely. The Fe inclusions in the substrate provide an increasing number of island nucleation sites, which accounts for the unusual increasing rate of island nucleation for $\theta \lesssim 0.3$ ML [Fig. 4(c)]. Initially, the number density of Fe inclusions is ~14 times greater than the number of first layer islands, but by $\theta = 0.3$ ML the densities are of the same order of magnitude. The presence of small islands even well after coalescence has begun [e.g., Fig 3(d)] shows that nucleation at Fe inclusions continues until the first layer is nearly complete.

Whereas the first Fe atoms form inclusions, once islands have nucleated arriving Fe atoms can follow an alternate kinetic path and aggregate at island boundaries. This new path predominates in the latter stages of first layer filling. Under the conditions when the STM is sensitive to composition, the aggregates of Fe at first layer boundaries bear the same apparent height relationship to the adjoining islands as the Fe inclusions bear to the Cu substrate.

We conclude therefore, that the mode of addition for arriving Fe atoms is determined by both surface composition and structure. On the bare Cu(100) substrate there is a thermodynamic driving force that leads to formation of the Fe inclusions. After first layer Cu islands nucleate, some Fe must arrive on these islands. The process of stepping down at edges and either adding at the island edge or exchanging with substrate Cu atoms predominates for small first layer islands. Nevertheless, a barrier to step crossing is expected to limit the rate at which arriving Fe atoms can step down. When first layer islands are sufficiently large, a high enough concentration of Fe atoms can build up on top of islands to nucleate second layer islands.

As the first layer fills, island shapes become more complex as seen in Figs. 3(b)–3(d). In Fig. 4(c), the density of first layer islands peaks near $\theta = 0.3$ ML. We define the coverage of peak island density at $\theta_C = 0.3$ ML. Below this coverage, most Fe atoms arriving on first layer islands add at the edge of first layer Cu islands. Fe inclusions within the interior of first layer islands are infrequently observed, indicating a kinetic preference for Fe atoms to instead step down at island edges. Second layer nucleation becomes more probable only as island areas increase. In Fig. 4(a), it can be seen that second layer growth begins slowly near θ_C. The important conclusion is that the first epitaxial layer is heterogeneous in composition and that the substrate on which it rests is also heterogeneous. First layer islands consist of a Cu core composed of the ejected Cu atoms, with a perimeter containing both Fe and Cu. Although the exact layer composition cannot be determined from the STM images discussed to this point, in the following section we show that oxygen adsorption can be used to decorate selectively the Fe component.

Second layer growth is significant only after first layer islands begin to coalesce at θ_C but does not predominate until a second threshold coverage is reached. That can be seen in the data for layer 2 filling in Fig. 4(a). The threshold is at $\theta \approx 0.8$ ML. The cause of this change in the growth process can be seen in the change between images Figs. 3(d) and 3(e). Near this coverage the first layer reaches a percolation threshold θ_P. First layer growth becomes interconnected across the terraces with some remaining unconnected smaller islands. At this point, Fe atoms arriving on top of first layer growth can sample a much greater area on top of the first layer before crossing the first layer edge barrier. This allows greater opportunity for Fe atoms to nucleate new islands in the second layer or to add to existing second layer islands. From Figs. 3(e) and 3(f), it is also evident that nucleation occurs predominantly near the first layer edges. This unusual nucleation behavior results from the heterogeneous composition of the first layer and the predominance of Fe at the edges. At θ_P, Fig. 4(a) shows that the slope of the filling curve for first layer growth becomes shallower as the second layer growth rate simultaneously increases. Until this coverage, the primary growth has occurred at first layer islands. But the formation of a percolation network in the first layer opens an alternate kinetic path for the addition of arriving Fe atoms. With this understanding, it becomes clear why the layer filling is not characterized by simple layer-by-layer growth. The resulting structure from this process is depicted qualitatively in Fig. 1(d).

The data in Fig. 4(a) show that the first and second layers grow in tandem until $\theta \approx 2.0$ ML. At this point, the third layer growth has just begun and continues as the predominant growth process until that layer is filled. The Fe epitaxy has changed to become much more layer-by-layer in nature. Near this coverage, diffraction experiments observe a recovery in intensity followed by the start of oscillatory behavior.[5–7]

Information directly available from the STM images includes surface fraction exposed at each layer of growth. Using this measurement we calculate a layer structure factor using the following summation rule:

$$S_{\text{layer}} = \sum_{L=0}^{\infty} (-1)^L E_L .$$

In this summation, the exposed layer surface fraction for layer L is E_L. The layer structure factor S_{layer} is plotted for the measured data in Fig. 4(b). The square of S_{layer} can serve as a predictor for antiphase diffraction intensity, and in fact the minimum in actual measured diffraction intensity observed at $\theta \approx 1.0$ ML deposition[7] coincides with a zero crossing in our S_{layer} derived from the image data. Additionally, the beginning of layer-by-layer growth behavior after $\theta \cong 2.0$ ML causes S_{layer} to oscillate as is also observed by diffraction. A better comparison with diffraction experiments will take into account effects of coherence and length scales of surface structure.

With these and previous results from Fe deposition on Cu(100) for $\theta \leqslant 4$ ML, we are able to understand the atomic mechanisms of epitaxial growth for this system and explain previously contradictory results. Submonolayer growth exhibits intermixing in the top layer of the substrate. This gives rise to Fe atoms covered by mixed Fe and Cu first layer growth, and explains the observed forward-scattering anisotropies in XPD[3] and AED.[2] The apparent bilayer growth is actually the Fe inclusions in the substrate covered by first layer Cu islands. The unusual behaviors of electron[5,6] and atom diffraction[7] intensities during deposition are explained by the changing modes of Fe atom addition. The antiphase diffraction intensity can be partially explained by a layer structure factor S_{layer}, which is directly calculated from layer statistics measured in STM images.

IV. EFFECT OF O_2 EXPOSURE

We have investigated the changes in surface topography caused by oxygen exposure for Fe films with coverage

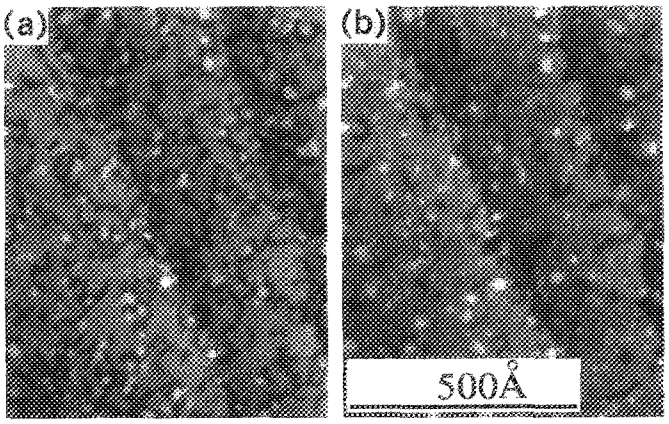

FIG. 6. Changes induced by oxygen exposure after deposition of $\theta = 0.66$ ML Fe. (a) $i_{\text{tunnel}} = 0.6$ nA, $V_{\text{sample}} = -1.5$ V. (b) Same region after exposure to 30 L O_2. $i_{\text{tunnel}} = 0.6$ nA, $V_{\text{sample}} = -1.5$ V.

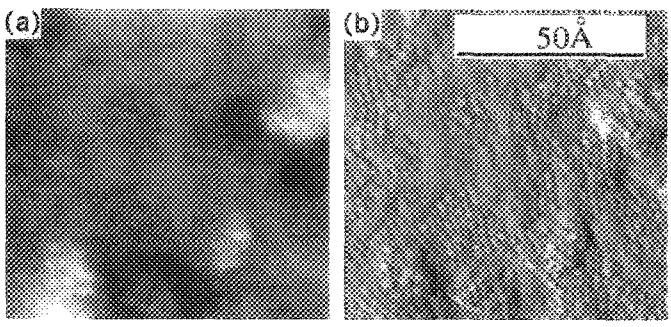

FIG. 7. Decoration of first layer Fe by exposure to oxygen. Note core of first layer growth consisting of ejected substrate Cu atoms does not show the strong corrugation observed at the perimeter, which is mostly Fe. Second layer growth is uniformly corrugated. (a) STM height image. $i_{\text{tunnel}} = 1.0$ nA, $V_{\text{sample}} = +50$ mV. (b) One-dimensional differentiated image emphasizing corrugation without layer height information.

$\theta < 1.0$ ML. For $\theta \cong 0.66$ ML Fe deposition, Fig. 6 shows the same surface area before and after exposure to ~ 30 L ($1\ \text{L} = 1 \times 10^{-6}$ Torr s)O_2. Comparing Figs. 6(a) and 6(b), the fraction of surface area filled by the first layer has increased by $\approx 25\%$. When we repeatedly expose samples with lower Fe coverages to O_2 in 5–10 L aliquots, we observe apparent growth of individual first layer islands after each exposure.[12] In Fig. 6(b), the size of second layer islands has also increased, but some second layer islands present before O_2 exposure are absent. Apparently the oxidation has promoted the step crossing of second layer islands near the edge of first layer growth, contributing partially to the increased filling of the first layer. However, this alone does not account for the increased coverage of the first layer. The manifestations of O_2 exposure on the layer filling of epitaxial growth depend strongly on the existing layer structure. Oxidation of an initial $\theta \cong 0.93$ ML Fe deposition showed considerably less apparent growth of the first layer area at a 6% increase in area. The area expansion of islands and interconnected growth indicates a structural change, rather than simple adsorption of oxygen on existing material. X-ray photoelectron spectroscopy indicates the formation of an iron oxide species on the surface.

The compositional heterogeneity of first layer growth is revealed by the atomic structure imaged in Fig. 7(a). A sample with $\theta \cong 0.93$ ML Fe deposited was exposed to ≈ 20 L O_2. Three levels are present in the image. The lowest is the original Cu substrate with no atomic scale structure resolved. First layer growth appears at intermediate height. The image clearly reveals regions at this level with atomic scale corrugation of ≈ 0.4 Å. But in the Cu core of the coalesced first layer network this structure is absent. At the highest level in this image are islands of second layer growth, which consistently show similar corrugation, but with larger lateral size. Figure 7(b) enhances the appearance of the corrugation by a one-dimensional differentiation. The first layer corrugation consists of domains with rectangular symmetry in two orientations, but poor ordering within domains. The unit cell size measured is too large for simple iron–iron spacings, leading us to conclude that the structure is from an iron oxide formed by the oxygen exposure.

Exposure of the Cu(100) substrate to O_2 prior to Fe deposition is known to change the layer-by-layer behavior of Fe epitaxy.[3] We have imaged submonolayer Fe epitaxy on a preoxidized Cu(100) substrate and have not observed the patches imaged after deposition on the clean Cu(100) substrate. Unfortunately, the resulting surface structure appears unstable at room temperature, or possibly more susceptible to background gas contamination, and our images of the surface change with time. This precludes an accurate measurement of layer statistics at least for $\theta \lesssim 0.8$ ML.

V. CONCLUSIONS

By imaging a series of Fe coverages on Cu(100) with $\theta < 3.0$ ML, we measured layer coverage statistics as a function of the amount of Fe deposited. The layer filling behavior changes with the evolving surface composition and structures. Initially, the Cu substrate is modified by atom exchange and formation of Fe inclusions. The inclusions are imaged by STM with an unusual and unexplained sensitivity to composition. First layer islands of the ejected Cu nucleate at these inclusions and partially cover the Fe. Eventually, Fe begins to add to the edge of these Cu first layer islands. As growth proceeds the resulting first layer structure changes; islands coalesce followed by the formation of a percolation network, both of which promote the growth of second layer Fe. First and second layer growth approach completion nearly simultaneously, after which images reveal layer-by-layer growth mode. This continues until the substrate stabilization of fcc Fe yields to the bcc bulk structure at $\theta \approx 10$ ML. A STM study of this latter growth transition is in progress.

Adsorbed oxygen alters the layer filling by two means. First, second layer growth near step edges crosses to add at the edge of first layer growth, and second, the apparent area of the deposited layer is expanded by formation of an iron oxide species.

ACKNOWLEDGMENT

This work was supported in part by the Office of Naval Research (N00014-89-C-0099).

[1]M. Onellion, M. A. Thompson, and J. L. Erskine, Surf. Sci. **179**, 219 (1987).
[2]S. A. Chambers, T. J. Wagener, and J. H. Weaver, Phys. Rev. B **36**, 8992 (1987).
[3]D. A. Steigerwald, I. Jacob, and W. F. Egelhoff, Jr., Surf. Sci. **202**, 472 (1988).
[4]H. Glatzel, Th. Fauster, B. M. U. Scherzer, and V. Dose, Surf. Sci. **254**, 58 (1991).
[5]D. A. Steigerwald and W. F. Egelhoff, Jr., Surf. Sci. **192**, L887 (1987).
[6]J. Thomassen, B. Feldman, and M. Wuttig, Surf. Sci. **264**, 406 (1992).
[7]M. Arnott, E. M. McCash, and W. Allison, Surf. Sci. **269**, 724 (1992).
[8]S. Rousset, S. Chiang, D. E. Fowler, and D. D. Chambliss, Phys. Rev. Lett. **69**, 3200 (1992).
[9]S. Chiang, R. J. Wilson, C. Gerber, and V. M. Hallmark, J. Vac. Sci. Technol. A **6**, 386 (1988).
[10]D. D. Chambliss, R. J. Wilson, and S. Chiang, J. Vac. Sci. Technol. A **10**, 1993 (1992).
[11]D. D. Chambliss and S. Chiang, Surf. Sci. Lett. **264**, L187 (1992).
[12]K. E. Johnson, D. D. Chambliss, S. Chiang, and R. J. Wilson (unpublished).